Structural Engineering and Mechanics, *Vol. 68, No. 3 (2018) 325-334*
DOI: https://doi.org/10.12989/sem.2018.68.3.325

Analytical, numerical and experimental investigation of low velocity impact response of laminated composite sandwich plates using extended high order sandwich panel theory

Sattar Jedari Salami*[1] and Soheil Dariushi[2a]

[1]*Department of Mechanical Engineering, Damavand Branch, Islamic Azad University, Damavand, Iran*
[2]*Department of Composite, Iran Polymer and Petrochemical Institute, Tehran-Karaj Highway, Pajuhesh Boulevard, Tehran, Iran*

(Received March 26, 2018, Revised September 11, 2018, Accepted September 12, 2018)

Abstract. The Nonlinear dynamic response of a sandwich plate subjected to the low velocity impact is theoretically and experimentally investigated. The Hertz law between the impactor and the plate is taken into account. Using the Extended High Order Sandwich Panel Theory (EHSAPT) and the Ritz energy method, the governing equations are derived. The skins follow the Third order shear deformation theory (TSDT) that has hitherto not reported in conventional EHSAPT. Besides, the three dimensional elasticity is used for the core. The nonlinear Von Karman relations for strains of skins and the core are adopted. Time domain solution of such equations is extracted by means of the well-known fourth-order Runge-Kutta method. The effects of core-to-skin thickness ratio, initial velocity of the impactor, the impactor mass and position of the impactor are studied in detail. It is found that these parameters play significant role in the impact force and dynamic response of the sandwich plate. Finally, some low velocity impact tests have been carried out by Drop Hammer Testing Machine. The results are compared with experimental data acquired by impact testing on sandwich plates as well as the results of finite element simulation.

Keywords: sandwich plate; low velocity impact; extended high order sandwich panel theory; geometrical nonlinearity; experiment

1. Introduction

Sandwich structures are made up of two thin but strong face sheets and one thick but lightweight core. Sandwich structures are designed to provide superior bending stiffness and in-plane stability at low specific weights (Block 2014). There are lots of theories and models that have been presented to explain the behavior of sandwich structures under different loading conditions (Abrate *et al.* 2017, Ahmadi 2018, Ying *et al.* 2017, El-Haina*et al.* 2017, Caliri *et al.* 2016, Elmossouess *et al.* 2017).

Frostig *et al.* (1992) presented the famous high order sandwich panel theory (HSAPT) that combined the equivalent single layer (ESL) theories and elasticity one for analyzing sandwich panels. Since the thickness of face sheets is so much lower than the core, faces follow ESL theories such as classic beam or plate theories. Therefore, the transverse stress components of the face sheets are neglected and the core is considered as a three dimensional medium assuming that the in plane stress components of the core are omitted due to its softness in the in-plane directions. To date, HSAPT has been improved based on modification of theoretical assumptions that firstly considered for the face sheets and the core (Frostig *et al.* 2013, Elmalich and Rabinovitch 2012, Livani *et al.* 2016, Malekzadeh and Livani 2015, Malekzadeh 2014) On the other hand, the HSAPT has been enhanced geometrically to increase the accuracy of analyzing the sandwich panels under large deformations.So, some of studied dealing with nonlinear HSAPT have been presented that indicate large deformations with moderate rotations for face sheets (Von-Karman strain) while the core follow small deformation assumption (Hamed and Frostig 2015, Yuan and Kardomateas 2015). Sokolinsky and Frostig (1999) and Sokolinsky *et al.* (2000) studied nonlinear buckling response of Sandwich beam based on HSAPT. As it is necessary to consider geometrically nonlinearity for buckling analysis, the face sheets follow Von- Karman strain assumptions while the strains of the core is approximated based on small strain theory.

Also, a few references considered large deformation for the core because of the particular conditions of the loading (Hohe and Librescu 2003, Frostig *et al.* 2005, Dariushi and Sadighi 2014, Yuan *et al.* 2016). Frostig *et al.* (2005) investigated the nonlinear bending response of sandwich beams, considering Von- Karman strains for the faces and large strains for the core. The governing equations that obtained from HSAPT are very complicated. Two assumptions are carried out to simplify the equations. At first, the nonlinearity of the core is considered only for the shear angle. Secondly, the strains of the core follow the linear kinematic relations. The study shows that two methods receive nearly the same results.

Eventually, by improvement of the HSAPT, Phan *et al.*

*Corresponding author, Assistant Professor
E-mail: sattar.salami@aut.ac.ir
[a]Assistant Professor
E-mail: s.dariushi@ippi.ac.ir

ISSN: 1225-4568 (Print), 1598-6217 (Online)

(2012a) formulated a new high order theory for sandwich panels. This theory is an extension of the HSAPT and includes the in-plane stress components of the core. It was proven, by comparison to the elasticity solution that this approach results in superior accuracy, especially for the cases of stiffer cores, for which cases the HSAPT cannot predict correctly the stress fields involved. Thus, this theory, referred to as the "extended high-order sandwich panel theory" (EHSAPT). Also, the geometrically nonlinear EHSAPT is applied for bending analysis of a sandwich beam based on nonlinear Von- Karman strains of the face sheets while the strains of the core remained small Phan *et al.* (2012b). With a few improvements of the EHSAPT, face sheets are analyzed based on the first order shear deformation theory (FSDT) to study the response of a sandwich panel with bilinear constitutive behavior for shear stress of the core (Salami *et al.* 2014). This theory is called improved extended high order sandwich panel theory (IEHSAPT). Besides, by enhancing one step of this theory, third order shear deformation theory (TSDT) is applied to face sheets in the new improved HSAPT and biaxial buckling of sandwich plate is investigated (Kheirikhah *et al.* 2012). Strain- displacement relations of the face sheets and the core follow nonlinear Von-Karman strains. The results show the solution from the current theory is very close to elasticity solution.

To date, only few works dealing with investigation of low velocity impact behavior of sandwich plates have been presented based on HSAPT.

High order impact analysis of sandwich structures with flexible core was first presented by Yang and Qiao (2005). They formulated the impact process based on the higher-order model and analyzed local deflection and stress concentration effects of the impact. The core was considered as a two dimensional elastic medium and the skins follow classical beam theory. Small strain hypothesis are used for the skins and the core.

In another study, Qiao and Yang (2007) used the HSAPT to study vibration and impact behavior of large scale fiber reinforced polymer structural honeycomb composite sandwich beams with sinusoidal core geometry. Yang and Qiao (2007) also studied the effect of asymmetric lay up of sandwich beams with arbitrary boundary conditions. Finite difference method (FDM) is used to solve the governing equations. The effect of joint-joint supported and clamped boundaries on impact response is discussed.

Malekzadeh *et al.* (2006) improved the model that has been proposed by Yang and Qiao (2005) by considering first order shear deformation theory (FSDT) for face sheets. Low velocity impact dynamic of a composite sandwich panel with transversely flexible core is analyzed and multiple small impactors with small masses are assumed. The kinematic relations for face sheets and core were based on small deformation and rotations. Also, the fully dynamic effects of all constituents are considered.

As the above literature survey accepts, and to the best of author's knowledge, there is no work on the low velocity impact response of a sandwich panel based on nonlinear EHSAPT. Present study aims to fill this gap in the open literature. To this purpose, low velocity impact analysis of a sandwich plate based on the new improved EHSAPT is investigated. The TSDT is used for face sheets and transverse and in-plane normal strains and stresses of the core are considered. Also, the nonlinear Von-Karman type relations are used to obtain strains. The governing equations are derived via the Ritz based applied to the total energy of the system. The influences of the core-to-skin thickness ratio, initial velocity of the impactor, mass of impactor and the contact position of the impactor are studied in details.

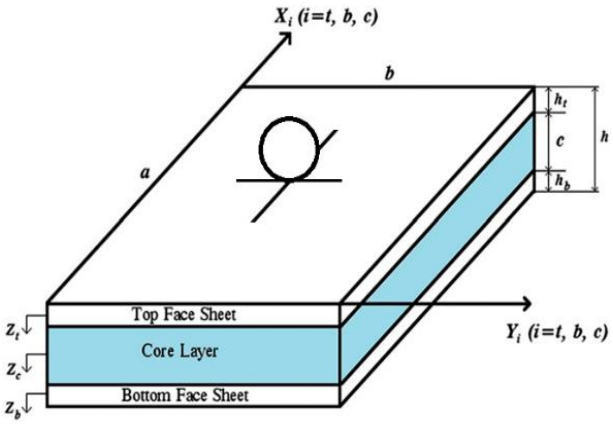

Fig. 1 Description of the geometrical configuration for the sandwich plate

2. Analytical formulation

A sandwich rectangular plate which has a length "a", width "b", and total thickness "h" is considered. Geometry and coordinate systems are shown in Fig. 1. The sandwich is formed from top and bottom skins and the core layer. All parts are assumed with uniform thickness and the z coordinate of each part is measured downward from its mid-plane. Third-order shear deformation plate theory (TSDT) is applied in formulation of the skins in this study. As a result of this, cubic function is assumed for in-plane displacements and transverse inextensibility is considered. Since the transverse shear strains vary parabolically through the skin thickness in TSDT, it coincides with actual shear stress distribution. In this research, compressibility of the soft core in the transverse direction is also considered. Hence, the transverse displacement in the core is of second order in the transverse coordinate and the in-plane displacements are of third order in the transverse coordinate. The geometrically nonlinear Von-Karman relations are taken into account to obtain strains.

2.1 Skins

The displacement components of the top and bottom skins are formulated based on third order shear deformable theory (Reddy 2006). Therefore, in-plane and transverse displacement components, i.e., u^i, v^i and w^i may be written in terms of in-plane displacements of mid-plane $u^i{}_0$ and $v^i{}_0$, transverse displacement of the mid-plane $w^i{}_0$, and φ^i and ψ^i rotations of cross sections about the y and x axes, respectively, as

$$\begin{aligned} u^i(x,y,z,t) &= u_0^i(x,y,t) + z_i\varphi^i(x,y,t) - C_s z_i^3(\varphi^i + w_{0,x}^i) \\ v^i(x,y,z,t) &= v_0^i(x,y,t) + z_i\psi^i(x,y,t) - C_s z_i^3(\psi^i + w_{0,y}^i) \\ w^i(x,y,z,t) &= w_0^i(x,y,t) \end{aligned} \tag{1}$$

In which $C_s=4/3h_i^2$ to consider quadratic variation of transverse shear strains and satisfy the vanishing of them on the top and bottom surfaces of the skins. Superscript (*i=t or b*) refers to top and bottom skins. Based on nonlinear Von-Karman kinematic relations

$$\begin{aligned} \varepsilon_{xx}^i &= u_{0,x}^i + \frac{1}{2}\left(w_{0,x}^i\right)^2 + z\phi_{,x}^i - \\ & C_s z^3(\phi_{,x}^i + w_{0,xx}^i) \end{aligned} \tag{2}$$

$$\begin{aligned} \varepsilon_{yy}^i &= v_{0,y}^i + \frac{1}{2}\left(w_{0,y}^i\right)^2 + z\psi_{,y}^i - \\ & C_s z^3(\psi_{,y}^i + w_{0,yy}^i) \end{aligned} \tag{3}$$

$$\begin{aligned} \gamma_{yz}^i &= v_{,z}^i + w_{,y}^i = \\ & (1-3C_s z_i^2)(\psi^i + w_{0,y}^i) \end{aligned} \tag{4}$$

$$\begin{aligned} \gamma_{xz}^i &= u_{,z}^i + w_{,x}^i = \\ & (1-3C_s z_i^2)(\varphi^i + w_{0,x}^i) \end{aligned} \tag{5}$$

$$\begin{aligned} \gamma_{xy}^i &= u_{0,y}^i + v_{0,x}^i + \frac{1}{2}\left(w_{0,x}^i w_{0,y}^i\right) + \\ & z_i(\varphi_{,y}^i + \psi_{,x}^i) - C_s z_i^3(\varphi_{,y}^i + \psi_{,x}^i + 2w_{0,xy}^i) \end{aligned} \tag{6}$$

As the top and bottom skins are considered transversely isotropic laminates the stress-strain relations can be defined as

$$\begin{bmatrix} \sigma_{xx}^i \\ \sigma_{yy}^i \\ \tau_{yz}^i \\ \tau_{xz}^i \\ \tau_{xy}^i \end{bmatrix} = \begin{bmatrix} \bar{C}_{11} & \bar{C}_{12} & 0 & 0 & \bar{C}_{16} \\ \bar{C}_{12} & \bar{C}_{22} & 0 & 0 & \bar{C}_{26} \\ 0 & 0 & \bar{C}_{44} & \bar{C}_{45} & 0 \\ 0 & 0 & \bar{C}_{45} & \bar{C}_{55} & 0 \\ \bar{C}_{16} & \bar{C}_{26} & 0 & 0 & \bar{C}_{66} \end{bmatrix} \begin{bmatrix} \varepsilon_{xx}^i \\ \varepsilon_{yy}^i \\ \gamma_{yz}^i \\ \gamma_{xz}^i \\ \gamma_{xy}^i \end{bmatrix} \tag{7}$$

Where $\bar{C}_{mn}$ (m,n=1,2,4,5,6) are transformed stiffness coefficients and defined in reference books (e.g., Reddy 2006)

2.2 Core

The vertical and longitudinal displacements of core are assumed as cubic and quadratic polynomials in the transverse direction, respectively.

$$\begin{aligned} w^c(x,y,z,t) &= w_0^c(x,y,t) + \\ & w_1^c(x,y,t)z_c + w_2^c(x,y,t)z_c^2 \end{aligned} \tag{8}$$

$$\begin{aligned} u^c(x,y,z,t) &= u_0^c(x,y,t) + \\ & \varphi_0^c(x,y,t)z_c + u_2^c(x,y,t)z_c^2 \\ & + u_3^c(x,y,t)z_c^3 \end{aligned} \tag{9}$$

$$\begin{aligned} v^c(x,y,z,t) &= v_0^c(x,y,t) + \\ & \psi_0^c(x,y,t)z_c + v_2^c(x,y,t)z_c^2 \\ & + v_3^c(x,y,t)z_c^3 \end{aligned} \tag{10}$$

Where "c" superscript refers to core, "w_0" and "u_0" are the transverse and in-plane displacements; "φ_0" and "ψ_0" are the slope at the mid plane of the core about the y and x axes, respectively. In this study, the core is perfectly bonded to the skins. Hence, transverse and in-plane compatibility conditions in upper (z=-c/2), and lower (z=c/2) skin-core interfaces which can be obtained as follows

$$w^c(x,y,-\frac{c}{2},t) = w^t(x,y,\frac{d_t}{2},t) \tag{11}$$

$$u^c(x,y,-\frac{c}{2},t) = u^t(x,y,\frac{d_t}{2},t) \tag{12}$$

$$v^c(x,y,-\frac{c}{2},t) = v^t(x,y,\frac{d_t}{2},t) \tag{13}$$

$$w^c(x,y,\frac{c}{2},t) = w^t(x,y,-\frac{d_b}{2},t) \tag{14}$$

$$u^c(x,y,-\frac{c}{2},t) = u^t(x,y,-\frac{d_b}{2},t) \tag{15}$$

$$v^c(x,y,\frac{c}{2},t) = v^t(x,y,-\frac{d_b}{2},t) \tag{16}$$

Using Eqs. (8) to (10) the coefficients (w_1, w_2 and u_2, u_3) are analytically determined in terms of the displacement components of skins, mid plane displacement components and the slope at the mid plane of the core. Finally, after some algebraic manipulations the transverse and in-plane displacements of the core can be written as follows

$$\begin{aligned} w^c(x,y,z,t) &= w_0^c + \frac{1}{c}\left[w_0^b - w_0^t\right]z_c \\ & + \frac{2}{c^2}\left[w_0^t + w_0^b - 2w_0^c\right]z_c^2 \end{aligned} \tag{17}$$

$$\begin{aligned} u^c(x,y,z,t) &= u_0^c + \varphi_0^c z_c + \\ & \frac{2z_c^2}{c^2}\begin{pmatrix} u_0^t + u_0^b - 2u_0^c + \frac{d_t}{2}\varphi^t - \frac{d_b}{2}\varphi^b \\ -\frac{d_t}{6}(\varphi^t + w_{0,x}^t) + \frac{d_b}{6}(\varphi^b + w_{0,x}^b) \end{pmatrix} + \\ & \frac{4z_c^3}{c^3}\begin{pmatrix} -u_0^t - \frac{d_t}{2}\varphi^t - \frac{d_b}{2}\varphi^b + u_0^b - c\varphi_0^c + \\ \frac{d_t}{6}(\varphi^t + w_{0,x}^t) + \frac{d_b}{6}(\varphi^b + w_{0,x}^b) \end{pmatrix} \end{aligned} \tag{18}$$

$$v^c(x,y,z,t) = v_0^c + \psi_0^c z_c + \frac{2z_c^2}{c^2}\begin{pmatrix} v_0^t + v_0^b - 2v_0^c + \frac{d_t}{2}\psi^t - \frac{d_b}{2}\psi^b \\ -\frac{d_t}{6}(\psi^t + w_{0,y}^t) + \frac{d_b}{6}(\psi^b + w_{0,y}^b) \end{pmatrix} + \frac{4z_c^3}{c^3}\begin{pmatrix} -v_0^t - \frac{d_t}{2}\psi^t - \frac{d_b}{2}\psi^b + v_0^b - c\psi_0^c \\ +\frac{d_t}{6}(\psi^t + w_{0,y}^t) + \frac{d_b}{6}(\psi^b + w_{0,y}^b) \end{pmatrix} \quad (19)$$

The Von-Karman strain-displacement relations for the core can be defined as

$$\varepsilon_{xx}^c = u_{,x}^c + \frac{1}{2}\left(w_{,x}^c\right)^2 \quad (20)$$

$$\varepsilon_{yy}^c = v_{,y}^c + \frac{1}{2}\left(w_{,y}^c\right)^2 \quad (21)$$

$$\varepsilon_{zz}^c = w_{,z}^c \quad (22)$$

$$\gamma_{xy}^c = u_{,y}^c + v_{,x}^c + w_{,x}^c w_{,y}^c \quad (23)$$

$$\gamma_{yz}^c = v_{,z}^c + w_{,y}^c \quad (24)$$

$$\gamma_{xz}^c = u_{,z}^c + w_{,x}^c \quad (25)$$

After applying Eqs. (17) to (19) into Eqs. (20) to (25) the strain-displacement relations based on independent variables can be obtained. The stress- strain relationships for the isotropic core can be read as follows

$$\begin{bmatrix} \sigma_{xx}^c \\ \sigma_{yy}^c \\ \sigma_{zz}^c \\ \tau_{yz}^c \\ \tau_{xz}^c \\ \tau_{xy}^c \end{bmatrix} = \frac{E(1-\nu)}{(1+\nu)(1-2\nu)}[A]\begin{bmatrix} \varepsilon_{xx}^c \\ \varepsilon_{yy}^c \\ \varepsilon_{zz}^c \\ \gamma_{yz}^c \\ \gamma_{xz}^c \\ \gamma_{xy}^c \end{bmatrix}$$

$$[A] = \begin{bmatrix} 1 & \frac{\nu}{1-\nu} & \frac{\nu}{1-\nu} & 0 & 0 & 0 \\ \frac{\nu}{1-\nu} & 1 & \frac{\nu}{1-\nu} & 0 & 0 & 0 \\ \frac{\nu}{1-\nu} & \frac{\nu}{1-\nu} & 1 & 0 & 0 & 0 \\ 0 & 0 & \frac{1-2\nu}{2(1-\nu)} & 0 & 0 & 0 \\ 0 & 0 & 0 & \frac{1-2\nu}{2(1-\nu)} & 0 & 0 \\ 0 & 0 & 0 & 0 & \frac{1-2\nu}{2(1-\nu)} & 0 \end{bmatrix} \quad (26)$$

The stress-displacement relations can be expressed by inserting the strain-displacement relations in Eq. (26). This in turn, all strain and stress components resulted in terms of displacements.

2.3 Dynamics of contact region

Based on an investigation developed by Abrate (2005) the impact load applied by a spherical impactor may be related to the indentation value of the top skin through the following Hertzian contact law.

$$F(t) = K_h \alpha^{3/2} \quad (27)$$

Where α is the indentation value between the impactor and the top skin. Therefore, it is defined as

$$\alpha = w_p - w^t\left(\frac{a}{2}, \frac{b}{2}, -\frac{d_t}{2}\right) \quad (28)$$

Where w_p indicates the displacement of impactor, and $w_t(a/2, b/2, -dt/2)$ is the transverse displacement of the top skin at the impact position. Also, the impact stiffness is

$$K_h = \frac{4}{3}Q_\alpha\sqrt{R} \quad (29)$$

R is the indenter tip radius and $Q\alpha$ is defined as

$$\frac{1}{Q_\alpha} = \frac{1-\nu_{zs}^2}{E_{zs}} + \frac{1-\nu_{zi}^2}{E_{zi}} \quad (30)$$

E_z is the elastic modulus in the transverse direction and υ_z is Poisson's ratio of the skin (s) or impactor (i). Since the stiffness of the impactor is much more than that of the skin, Eq. (30) may be reduced to

$$\frac{1}{Q_\alpha} = \frac{1-\nu_{zs}^2}{E_{zs}} \quad (31)$$

2.4 Governing equations

The Ritz method is pursued to obtain governing equations of motion from total potential energy function of the sandwich plate. The total potential energy (Π) includes kinetic energy (T), strain energy (U) and potential of external works (W).

$$\prod = T + U + W \quad (32)$$

The strain energy of the sandwich beam that consists of stress and strain of face sheets and core, is given by

$$U = \int_{V_t}\left(\frac{1}{2}\sigma_{xx}^t\varepsilon_{xx}^t + \frac{1}{2}\sigma_{yy}^t\varepsilon_{yy}^t + \frac{1}{2}\tau_{yz}^t\gamma_{yz}^t + \frac{1}{2}\tau_{xz}^t\gamma_{xz}^t + \frac{1}{2}\tau_{xy}^t\gamma_{xy}^t\right)dv_t + \int_{V_c}\left(\frac{1}{2}\sigma_{xx}^c\varepsilon_{xx}^c + \frac{1}{2}\sigma_{yy}^c\varepsilon_{yy}^c + \frac{1}{2}\sigma_{zz}^c\varepsilon_{zz}^c + \frac{1}{2}\tau_{yz}^c\gamma_{yz}^c + \frac{1}{2}\tau_{xz}^c\gamma_{xz}^c + \frac{1}{2}\tau_{xy}^c\gamma_{xy}^c\right)dv_c + \int_{V_b}\left(\frac{1}{2}\sigma_{xx}^b\varepsilon_{xx}^b + \frac{1}{2}\sigma_{yy}^b\varepsilon_{yy}^b + \frac{1}{2}\tau_{yz}^b\gamma_{yz}^b + \frac{1}{2}\tau_{xz}^b\gamma_{xz}^b + \frac{1}{2}\tau_{xy}^b\gamma_{xy}^b\right)dv_b + \frac{2}{5}K_h(w_p - w^t(\frac{a}{2}, \frac{b}{2}, -\frac{d_t}{2})) \quad (33)$$

The kinetic energy of the system, considering both the kinetic energies of the sandwich panel and impactor. Thus, it can be written as

$$\begin{aligned} T &= \int_{V_t}\left(\frac{1}{2}\rho_t(\dot{u}_t^2+\dot{v}_t^2+\dot{w}_t^2)\right)dv_t \\ &+\int_{V_c}\left(\frac{1}{2}\rho_c(\dot{u}_c^2+\dot{v}_c^2+\dot{w}_c^2)\right)dv_c \\ &+\int_{V_b}\left(\frac{1}{2}\rho_b(\dot{u}_b^2+\dot{v}_b^2+\dot{w}_b^2)\right)dv_b \\ &+\frac{1}{2}M_p\dot{w}_P^2 \end{aligned} \tag{34}$$

Where ρ_t, ρ_b and $\rho_c$are the densities of the top face sheet, bottom face sheet and the core, respectively. Also, M_P indicates the mass of the impactor. The potential of external works equals to

$$W=-\int_0^t F(t)\,\mathrm{d}w_0 \tag{35}$$

Using Ritz method, the solution of the displacement variables should be assumed based on satisfying the essential boundary conditions. Thus, in case of simply supported plate, displacement functions of the skins and the core can be expressed in the following forms. Where Ω^i, represents the time dependent unknown coefficients according to assumed displacement functions. M is the number of terms should be selected to assure the convergence of the series functions.

$$\left\{\Omega^i(t)\right\}=\begin{Bmatrix}\left\{U^i_{mn}(t)\right\},\left\{V^i_{mn}(t)\right\},\\ \left\{\Phi^i_{mn}(t)\right\},\left\{\Psi^i_{mn}(t)\right\},\\ \left\{W^i_{mn}(t)\right\},\end{Bmatrix} \tag{36}$$

$$i=t,b,c,m=1...M,n=1...N$$

$$\begin{aligned} q^i(x,y,t)&=R^i_\delta R^i_\gamma\sum_{m=1}^{M}\sum_{n=1}^{N}\chi^i_{mn}(t)\\ \chi^i_{mn}(t)&=\Omega^i_{mn}(t)P^i_m(\xi)P^i_n(\eta)\end{aligned} \tag{37}$$

$$\begin{aligned} P_m(\xi)&=\cos[(m-1)\arccos(\xi)]\\ P_n(\eta)&=\cos[(n-1)\arccos(\eta)]\end{aligned} \tag{38}$$

In this study, Chebyshev polynomial (Upadhyay and Shukla 2013) type of shape functions are used. Here $P_m(\xi)$ and $P_n(\eta)$are one dimensional Chebyshev polynomials based to the non- dimensional parameters ξ and η. For coding and derivational convenience, the origin of the coordinate system is located at the center of the sandwich plate. So, ξ and η are introduced as $\xi=\frac{2x}{a}$, $\eta=\frac{2y}{b}$, where $\xi,\eta\in[-1,1]$. R_δ and R_γ are the functions that have to be chosen according to the essential boundary conditions. So, the functions can be written as Eqs. (39) and (40) for simply supported and clamped plate, respectively

$$\begin{aligned} &R_\delta=1-\xi^2\ ,(\delta=u_0^i(x,y,t),\\ &w_0^i(x,y,t),\varphi_0^i(x,y,t),\psi_0^i(x,y,t))\end{aligned} \tag{39}$$

$$\begin{aligned} &R_\gamma=1-\eta^2\ ,(\gamma=u_0^i(x,y,t),\\ &w_0^i(x,y,t),\varphi_0^i(x,y,t),\psi_0^i(x,y,t))\end{aligned} \tag{40}$$

Superscript i may denotes the top or bottom skins and the core. Substituting the Eq. (37) in to Eqs. (33) to (35) eliminates the dependency of the unknown variables to the spatial coordinates. Equations of motions then can be deduced based on the applying generalized Lagrange equations, as follows

$$\frac{\partial\prod}{\partial\Omega_i}=0\Rightarrow\frac{d}{dt}\left(\frac{\partial T}{\partial\dot{\Omega}_i}\right)+\frac{\partial U}{\partial\Omega_i}=-\frac{\partial W}{\partial\Omega_i} \tag{41}$$

The resulted equations from Eq. (41) is a system of nonlinear coupled ordinary differential equations. The set of equations in a matrix form, can be written as the follows

$$\begin{aligned} &[M]\left\{\ddot{\Omega}\right\}+\left[K\right]\left\{\Omega\right\}=\left\{F\right\}\\ &m_P\ddot{w}_P+F(t)=0\end{aligned} \tag{42}$$

Where [M] is mass matrix, [K] is a nonlinear coefficient matrix (or stiffness matrix) that depends upon unknown coefficients Ω^i, [F] is the force vector. The resulted nonlinear second order differential equations are then solved by the fourth-order Rung-Kutta method. The initial conditions for system of equations are as follows

$$\begin{cases}\Omega(t=0)=[0]\\ w_P(t=0)=0,\dot{w}_P(t=0)=V_0\end{cases} \tag{43}$$

3. Results and discussion

The results of present analysis which obtained from numerical solution of field equations are presented in this section. At first, results of analytical solution are compared with experimental and finite element results. Then, the effects of parametric studies are investigated to examine the influences of involved parameters on impact response of a sandwich plate with glass/epoxy composite skins and foam cores.

3.1 Comparison study

3.1.1 Experimental procedure

Low velocity impact tests were carried out on sandwich plates with composite skins. Composite skins were glass/epoxy (0-90-90-0-0-90-90-0) symmetric laminates

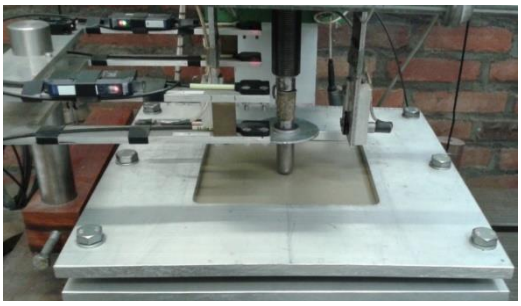

Fig. 2 Low velocity impact test on sandwich plate

Table 1 Material properties

Material	S2 glass/ FM94-epoxy prepreg	SAN foam
Young's modulus (GPa)	E_1=48.9, E_2= 5.5, E_3 =5.5	E=0.217
Shear modulus (GPa)	G_{12}=5.5, G_{13}=5.5 G_{23}=5	G=0.076
Density (Kg/m^3)	ρ=2000	ρ=210
Poisson's ratio	υ_{12}=0.33, υ_{13}=0.33 υ_{23}=0.0371	υ=0.42

with 1.2 mm thickness. The materials used for manufacturing of specimens with 1.2 mm thicknesses, unidirectional S2 glass/ FM94-epoxy prepreg and styrene acrylonitrile (SAN) foam (density=210 kg/m^3) from Gurit. Foam core thickness was 10mm for all specimens.

At first, composite skins were made by hand lay-up and were cured in autoclave for 3 hours at 6 bar pressure in temperature 120 ºc. The Skins were bonded to foam cores with 3M Scotch-Weld Epoxy Adhesive 2216 and cured in room temperature for 24 hours. Large panels were manufactured and then small specimens were cut in square shape with size of 12×12 cm^2.

Low velocity impact testes were carried out at the center of clamped specimens using instrumented drop weight tower (Fig. 2). The velocity of impactor nose was measured by two laser sensors with known distance. Impactor weight was constant (1000 gr) for all tests, therefore height of impactor controlled the impact velocity. A steel impactor with hemispherical nose with 8 mm radius was used. At least five specimen for each reported result were tested.

The elastic material properties of all components that have been used for manufacturing the specimens are tabulated in Table 1.

In order to validate the analytical model, sandwich plates with glass/epoxy composite faces subjected to low velocity impact is carried out using Drop Hammer Testing Machine in two contact velocities: 3 and 6 m/s. Fig. 4 shows comparisons of the contact force histories obtained from present theory and experimental results. As shown in Fig. 4, the peak value of contact force of experiment result is a little more than analytical one due to ignorance of surface stiffness in analytical model. Also, the main reasons of difference may be because of omitting the friction between supporters and specimens, ignoring the cohesive layers between skins and core and many defects occurred

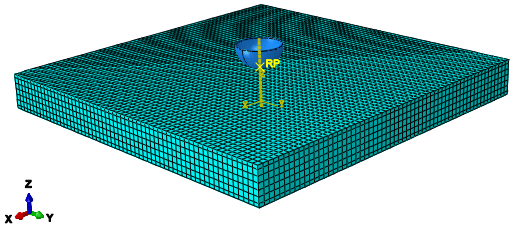

Fig. 3 Model of the sandwich plate and impactor in ABAQUS

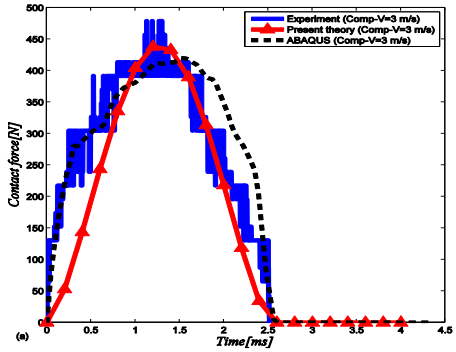

(a) V_0=3 m/s

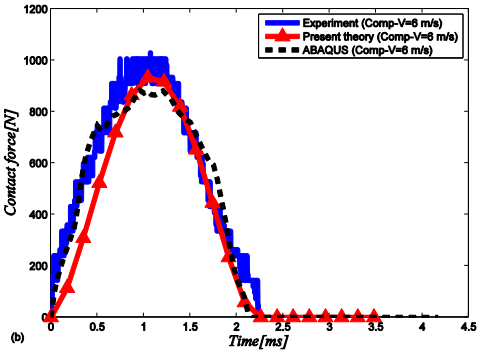

(b) V_0=6 m/s

Fig. 4 A comparison on contact force history of simply supported sandwich plate with foam core

during fabrication process that are not considered in theoretical formulation. It is obvious that there exist good agreement analytical and experimental results and the accuracy of analytical solution is verified.

3.1.2 Finite element modeling

To simulate the low velocity impact phenomenon, ABAQUS 6.14 is implemented. The model includes two parts as shown in Fig. 3. One is the impactor that is a hemispherical steel tip with radii of 8 mm. The mass and contact velocities of the projectile are the same with those of experimental procedure, i.e., M_0 = 1 Kg and V_0 = 3 and 6 m/s. The other part is a sandwich plate which has two laminated composite face sheets and the core with the same geometry with those used for test data and theoretical formulation. In order to define a kinetic energy for the projectile, a lumped mass will be assigned too one node called reference point (R.F.) on top of the finite element

mesh of the projectile. Since the properties of the composite laminated face sheets are considered transversely isotropic, the ENGINEERING CONSTANT option is applied in ABAQUS. Besides, to model the foam core as an elastic isotropic and homogeneous media in ABAQUS, the LINEAR ELASTIC option is applied for material properties. The whole target is modelled as a three dimensional media. The projectile is considered to be rigid and therefore the ANALYTICAL RIGID BODY characteristic is used for target modelling in ABAQUS. The mass and initial contact velocity of the projectile are assigned to the reference point. All edges of the target are clamped and the projectile is allowed to translate only in vertical direction. The face sheets are meshed by eight-node continuum shell element (SC8R) and solid element (C3D8R) is assigned for the core. The target is composed of 25200 elements and its mesh size is 2, according to a mesh sensitivity study to ensure that the results are converged reliably. The STEP option is used to model the loading and unloading processes during contact phase. As the type of loading is impact, the DYNAMIC EXPLICIT option is selected. A general contact condition is defined for the projectile and the target in the INTERACTION option of ABAQUS software package. Also, the CONSTRAINT RIGID BODY: Analytical surface is specified for projectile in the above option. In order to analyse the contact force of the target during the impact, a node under the point of impact is selected. The contact force histories obtained from the ABAQUS simulation are given in Fig. 4. The relative difference for the peak contact force, is about 3.5% and 5.5% for contact velocities 3 and 6 m/s, respectively, which are accepted in low velocity impact analysis. The main reasons of difference may be the present contact force model, local boundary conditions and divergence of flexural beam theories in comparison to the 3D case. It is seen that, the comparison is well justified which proofs the accuracy and efficiency of the developed method.

3.2 Parametric studies

The effects of essential parameters such as: core-to-skin thickness ratio, initial velocity of the impactor, the impactor mass and position of the impactor are investigated. The skins stacking sequence are symmetric cross ply (0/90/90/0/0/90/90/0) by considering 0.15 mm lamina thickness. The material properties of foam core and laminated composite skins are given in Table 1. Besides, material properties of the impactor and geometrical properties of the skins and the core are listed in Table 2.In order to study of inertia effects, several ratio of core to skin thicknesses are considered as given in Table 2. It should be noted that, the type of boundary conditions of sandwich plates are considered as simply supported.

3.2.1 Case I: Effect of the core-to-skin thickness ratio (c/ht)

The effect of core-to-skin thickness ratio (c/h_t) is demonstrated in Fig. 5. As may be conclude, increasing the core-to-skin thickness ratio has two opposite influences on the transverse displacement and contact force. In other words, the peak of contact force increases with the increase

Table 2 Material and geometrical properties of the impactor and sandwich plates

Impactor: R_{imp} = 15 *mm*(Radius) E_s=207 *GPa*, ρ_s=7960 kg/m^3 *and* υ_s=0.5
Skins: a=120 *mm*(Length), b=120 *mm* (Width), h_t=h_b=1.2(Thickness)
Core: C/h_t = 4, 6 and 8 (Core-to- skin thickness ratio)

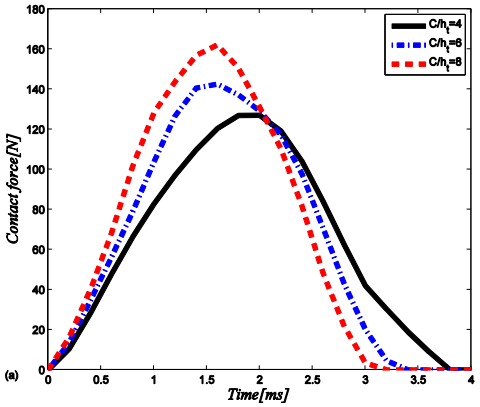

(a) Contact force history

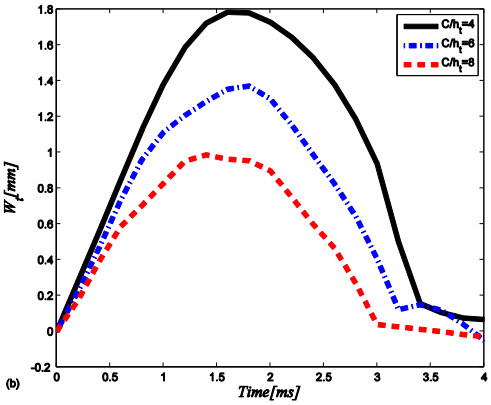

(b) Central transverse displacement

Fig. 5 The effect of core-to-skin thickness ratio(c/h_t) on low velocity impact responses at the mid-span point of the top skin

of c/h_t while the trend is inverse for the transverse displacement of the top face sheet. As the c/h_t increases, the thickness of the core increases which is expected since the sandwich plate becomes stiffer as flexural stiffness increases up.

3.2.2 Case II: Effect of initial velocity of impactor

The mass and initial velocity of the impactor are basic parameters that affected on the initial kinetic energy of the impactor. In this case, a simply supported sandwich plate is considered where core- to- skin thickness ratio is c/h_t=8. Results are depicted in Figs. 6 and 7. As concluded, the higher initial velocity of the impactor is, the higher peak contact force is. Besides, this parameter has little effect on contact time. Moreover, as the initial velocity of the impactor increases the transverse displacement of the mid-span increases.

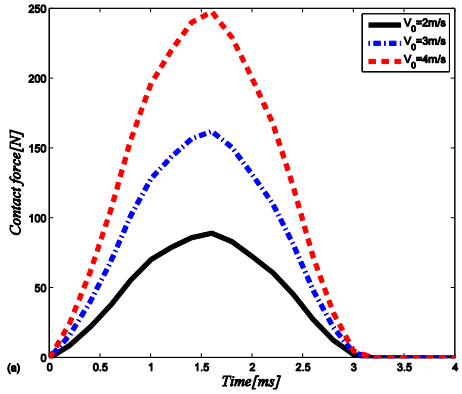

(a) Contact force history

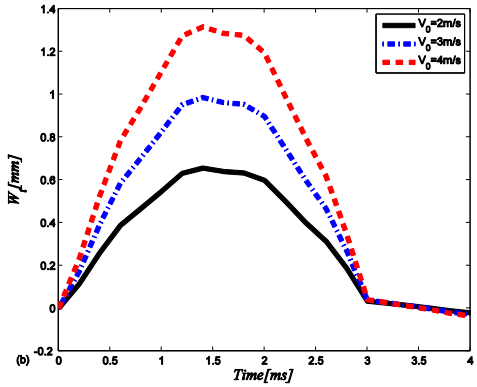

(b) Central transverse displacement

Fig. 6 The effect of initial velocity of the impactor on low velocity impact responses at the mid-span point of the top skin

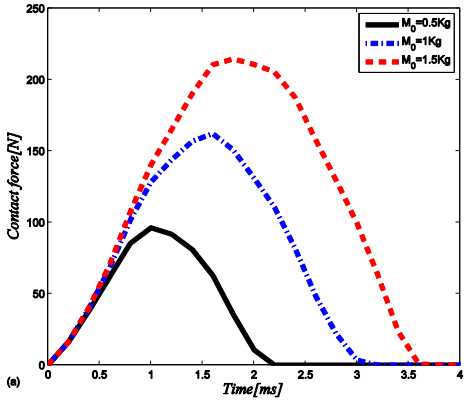

(a) Contact force history

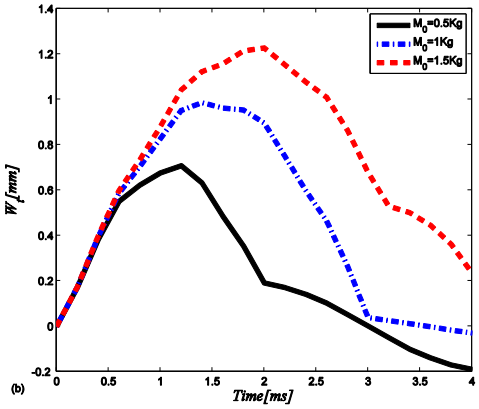

(b) Central transverse displacement

Fig. 7 Influence of the mass of the impactor on low velocity impact responses at the mid-span point of the top skin

3.2.3 Case III: Impactor mass effect

Another parameter that has significant role on kinetic energy is the mass of impactor. All properties of the model are the same with those applied in previous section. A S-S sandwich plate where core- to- skin thickness ratio c/h_t=8 is adopted. Initial velocity of the impactor is chosen as V_{imp}=3 m/s. In addition to M_0= 1 Kg, two other cases of M_0=0.5 Kg and M_0= 1.7 Kg are assumed. Since the impactor mass is the only variable, its influence on the dynamic response can be predicted in Fig. 6. As one may conclude, with increasing the impactor mass, the contact force is increased and also the contact time is increased. Therefore, the alternation of the contact time is similar to the contact force with respect to impactor mass. As expected, the transverse displacement of the top skin increases with increasing the impactor mass.

3.2.4 Case IV: Effect of impactor position

To investigate the effect of the impactor position, the sandwich plate with the same conditions of the previous sections is subjected under three different impact positions. The coordinates of the impact positions on the sandwich plates are (x_s = a/2, y_s=b/2), (x_s=a/8, y_s=b/8) and (x_s=a/16, y_s=b/16). Fig. 8 shows due to the higher local bending rigidity in the neighbourhood of the supported edges, the contact force increases, whereas the lateral deflection of the top skin decreases. In order to more clarity of results, the

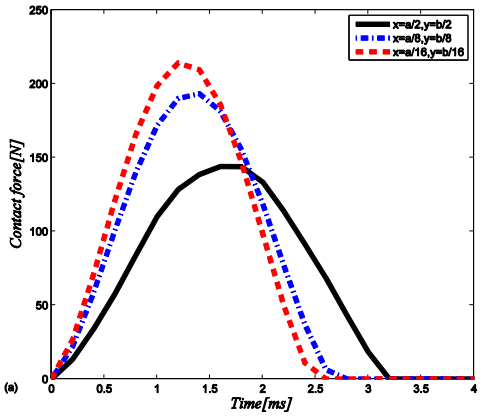

Fig. 8 The influence of impactor position on contact force of the top skin

three dimensional plots of the top skin deflections for three impact positions at the peak of contact are depicted in Fig. 9. Based on surface plots, as the impact position is closer to the supports, the peak of the deflection is decreased. In other words, as may be concluded, the highest peak of the deflection is belonging to the case subjected to impact at its mid span.

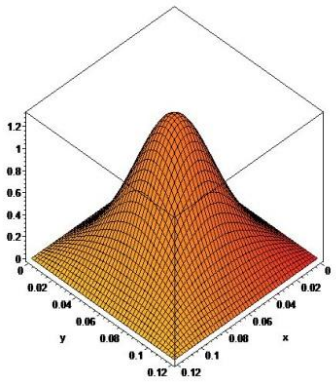

(a) x_s=a/2,y_s=b/2

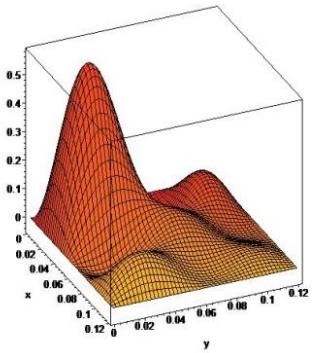

(b): x_s=a/8, y_s=b/8

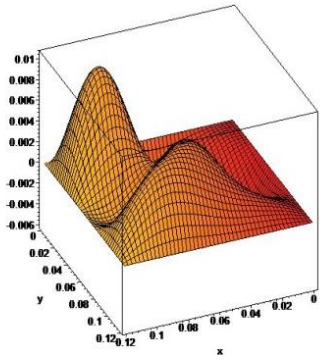

(c): x_s=a/16, y_s=b/16

Fig. 9 The influence of impactor position on top skin deflection at the peak of contact

4. Conclusions

In this research, nonlinear behavior of the sandwich plate with laminated composite skins and foam cores under low velocity impact is theoretically, numerically and experimentally studied. The Hertz contact law is applied to obtain contact force. The governing equations of the sandwich plate are achieved based on EHSAPT and the Ritz energy method. Besides, the fourth order Runge-Kutta method is carried out to solve the field equations in the time domain. The effects of core-to-skin thickness ratio, initial velocity of the impactor, the mass of impactor mass and position of the impactor are studied in detail. Therefore, the essential results are as follows:

• With increasing the core-to-skin thickness ratio, the peak of contact force increases while the trend is inverse for the transverse displacement of the top face sheet. As the c/h_t increases, the thickness of the core increases which is expected since the sandwich plate becomes stiffer as flexural stiffness increases up.

• Results indicates that the higher initial velocity of the impactor is, the higher peak contact force is. Besides, this parameter has little effect on contact time. Also, as the initial velocity of the impactor increases the transverse displacement of the midspan increases.

• As concluded, with increasing the impactor mass, the contact force is increased and also the contact time is increased. Therefore, the alternation of the contact time is similar to the contact force with respect to impactor mass. As expected, the transverse displacement of the top skin increases with increasing the impactor mass.

• It could be concluded that if the impact position is closer to the supports, the peak of the deflection is decreased. In other words, the highest peak of the deflection is belong to the case subjected to impact at its mid span. Due to the higher local bending rigidity in the neighbourhood of the supported edges, the contact force increases, whereas the lateral deflection of the top skin decreases.

• Generally, it is found that each of these parameters play significant role in the impact force and dynamic response of the laminated composite sandwich plates.

Acknowledgments

This work supported by Research Program supported by the Islamic Azad University, Damavand branch, Iran.

References

Abrate, S. (2005), *Impact on Composite Structures*, Cambridge University Press, New York, U.S.A.

Abrate, S. and Di Sciuva, M. (2017), "Equivalent single layer theories for composite and sandwich structures: A review", *Compos. Struct.*, **179**, 482-494.

Ahmadi, I. (2018), "Three-dimensional and free-edge hygrothermal stresses in general long sandwich plates", *Struct. Eng. Mech.*, **65**(3), 275-290.

Caliri, M., Ferreira, A. and Tita, V. (2016), "A review on plate and shell theories for laminated and sandwich structures highlighting the finite element method", *Compos. Struct.*, **156**, 63-77.

Dariushi, S. and Sadighi, M. (2014), "A new nonlinear high order theory for sandwich beam: An analytical and experimental investigation", *Compos. Struct.*, **108**, 779-788.

El-Haina, F., Bakora, A., Anis, A., Tounsi, B. and Mahmoud, S.R. (2017), "A simple analytical approach for thermal buckling of thick functionally graded sandwich plates", *Struct. Eng. Mech.*, **63**(5), 585-595.

Elmalich, D. and Rabinovitch, O. (2012), "A high-order finite element for dynamic analysis of soft-core sandwich plates", *J. Sandw. Struct. Mater.*, **14**(5), 525-555.

Elmossouess, B., Kebdani, S., Bouiadjra, M. and Tounsi, A. (2017), "A novel and simple HSDT for thermal buckling response of functionally graded sandwich plates", *Struct. Eng. Mech.*, **62**(4), 401-415.

Frostig, Y., Baruch, M., Vilnay, O. and Sheinman, I. (1992), "High

order theory for sandwich beam behavior with transversely flexible core", *J. Eng. Mech.*, **118**(5), 1026-1043.
Frostig, Y., Phan, C.N. and Kardomateas, G.A. (2013), "Free vibration of unidirectional sandwich panels, part I: Compressible core", *J. Sandw. Struct. Mater.*, **15**(4), 377-411.
Frostig, Y., Thomsen, O.T. and Sheinman, I. (2005), "On the non-linear high-order theory of unidirectional sandwich panels with a transversely flexible core", *Int. J. Sol. Struct.*, **42**(5-6), 1443-1463.
Hamed, E. and Frostig, Y. (2015), "Geometrically nonlinear creep behavior of debonded sandwich panels with a compliant core", *J. Sandw. Struct. Mater.*, **18**(1), 65-94.
Hohe, J. and Librescu, L. (2003), "A nonlinear theory for doubly curved anisotropic sandwich shells with transversely compressible core", *Int. J. Sol. Struct.*, **40**(5), 1059-1088.
Jedari Salami, S., Sadighi, M. and Shakeri, M. (2014), "Improved extended high orderanalysis of sandwich beams with a bilinear core shear behaviour", *J. Sandw. Struct. Mater.*, **16**(6), 633-668.
Kheirikhah, M.M., Khalili, S.M.R. and MalekzadehFard, K. (2012), "Biaxial buckling analysis of soft-core composite sandwich plates using improved high-order theory", *Eur. J. Mech. A-Sol.*, **31**(1), 54-66.
livani, M., MalekzadehFard, K. and Shokrollahi, S. (2016), "Higher order flutter analysis of doubly curved sandwich panels with variable thickness under aerothermoelastic loading", *Struct. Eng. Mech.*, **60**(1), 1-19.
Malekzadeh, K., Khalili, M.R., Olsson, R. and Jafari, A. (2006), "Higher-order dynamic response of composite sandwich panels with flexible core under simultaneous low-velocity impacts of multiple small masses", *Int. J. Sol. Struct.*, **43**(22-23), 6667-6687.
MalekzadehFard, K. (2014), "Higher order free vibration of sandwich curved beams with a functionally graded core", *Struct. Eng. Mech.*, **49**(5), 537-554.
MalekzadehFard, K. and Livani, M. (2015), "New enhanced higher order free vibration analysis of thick truncated conical sandwich shells with flexible cores", *Struct. Eng. Mech.*, **55**(4), 719-742.
Phan, C.N., Bailey, N.W., Kardomateas, G.A. and Battley, M.A. (2012), "Wrinkling of sandwich wide panels/beams based on the extended high-order sandwich panel theory: Formulation, comparison with elasticity and experiments", *Arch. Appl. Mech.*, **82**(10-11), 1585-1599.
Phan, C.N., Frostig, Y. and Kardomateas, G.A. (2012), "Analysis of sandwich beams with a compliant core and with in-plane rigidity-extended high order sandwich panel theory versus elasticity", *J. Appl. Mech.*, **79**(4), 041001.
Qiao, P. and Yang M. (2007), "Impact analysis of fiber reinforced polymer honeycomb composite sandwich beams", *Compos. Part B*, **38**(5-6), 739-750.
Reddy, J.N. (2006), *Theory and Analysis of Elastic Plates and Shells*, CRC Press, London, U.K.
Sokolinsky, V. and Frostig, Y. (1999), "Nonlinear behavior of sandwich panels with a transversely flexible core", *AIAA*, **37**(11), 1474-1482.
Sokolinsky, V. and Frostig, Y. (2000), "Branching behavior in the nonlinear response of sandwich panels with a transversely flexible core", *Int. J. Sol. Struct.*, **37**(40), 5745-5772.
Yang, M. and Qiao, P. (2005), "Higher-order impact modeling of sandwich structures with flexible core", *Int. J. Sol. Struct.*, **42**(20), 5460-5490.
Yang, M. and Qiao, P. (2007), "Impact and damage prediction of sandwich beams with flexible core considering arbitrary boundary effects", *J. Sandw. Struct. Mater.*, **9**(5), 411-444.
Ying, Z.G., Ni, Y.Q. and Duan, Y.F. (2017), "Stochastic vibration response of a sandwich beam with nonlinear adjustable visco-elastomer core and supported mass", *Struct. Eng. Mech.*, **64**(2), 259-270.
Yuan, Z. and Kardomateas, G.A. (2017), "Nonlinear dynamic response of sandwich wide panels", *Int. J. Sol. Struct.*, In Press.
Yuan, Z., Kardomateas, G.A. and Frostig, Y. (2016), "Geometric nonlinearity effects in the response of sandwich wide panels", *J. Appl. Mech.*, **83**(9), 91008.

CC